World Academy of Science, Engineering and Technology
International Journal of Mechanical and Mechatronics Engineering
Vol:7, No:1, 2013

Mode III Interlaminar Fracture in Woven Glass/Epoxy Composite Laminates

Farhad Asgari Mehrabadi, and Mohammad Reza Khoshravan

***Abstract*—**In the present study, fracture behavior of woven fabric-reinforced glass/epoxy composite laminates under mode III crack growth was experimentally investigated and numerically modeled. Two methods were used for the calculation of the strain energy release rate: the experimental compliance calibration (CC) method and the Virtual Crack Closure Technique (VCCT). To achieve this aim ECT (Edge Crack Torsion) was used to evaluate fracture toughness in mode III loading (out of plane-shear) at different crack lengths. Load–displacement and associated energy release rates were obtained for various case of interest. To calculate fracture toughness J_{III}, two criteria were considered including non-linearity and maximum points in load-displacement curve and it is observed that J_{III} increases with the crack length increase. Both the experimental compliance method and the virtual crack closure technique proved applicable for the interpretation of the fracture mechanics data of woven glass/epoxy laminates in mode III.

***Keywords*—**Mode III, Fracture, Composite, Crack growth Finite Element.

I. Introduction

During the last years it has been specified that the mode III delamination (tearing) is fundamental for the deep understanding of fracture characterization about composite laminates. The Crack Rail Shear (CRS) specimen is one of test method for characterizing mode III fracture toughness [1]. The drawback of CRS test is that the configuration has a low compliance and there is significant mode II contribution to the total stain energy release rate (SERR). Split Cantilever Beam (SCB) is another way to characterize mode III delamination fracture toughness used by [2], [3]. A modified version of the SCB specimen was developed by [4], [5] that due to use modified SCB (MSCB), eliminate some of the mode II component. Szekrényes [6] improved analysis of the MSCB test incorporating linear beam theories and expanded a closed form solution for the compliance and the energy release rate of the updated version of the mode III split-cantilever beam specimen.

In the last two decades, attempts to measure the mode III critical strain energy release rate (SERR) involved the Edge Crack Torsion (ECT) specimen [7], [8] such that, it is considered as a very important contribution to mode III fracture developments. Nonetheless, considerable research is still required to validate the ECT test for measuring J_{III} of laminated composites and crack growth behaving under out of plane shearing mode.

The main object of this paper is to develop a mode III tool for interlaminar fracture of woven fabric-reinforced glass/epoxy composite laminates using modified ECT fixture consisted of two support and two upper loading pins. In the present study, GFRP woven laminates were specially prepared and crack growth behavior under mode III were investigated. In addition, the possible fracture mode of delamination is discussed.

The strain energy release rate distribution along the delamination front is analyzed by using a three-dimensional finite element model and the mode I, mode II and mode III SERR component calculated by the virtual crack closure technique (VCCT). The validity of the ECT test for obtaining the mode III R-curve of woven glass/epoxy laminates was examined by comparing the experimental and numerical results.

II. Experimental Procedure

A. Material and Specimen

The specimens comprised 24 plies of Glass Satin Weave (SW) fabric (185 g/m2) of medium fiber volume fraction (around 40%) as the reinforcement and *ML506* (*Mokarrar®, IRAN*) epoxy resin was used to produce GFRP plate. Then a large panel was created with a lay-up sequence $[0/90]_{24}$ and a Teflon layer with a thickness of ~0.2 mm was inserted in the middle of the panel (i.e. between layer 12 and 13 of the fabric) to create the initial delamination. The panel was cured at room temperature overnight and then was cut into specimens. The specimens were aged for at least 10 days before testing. Fig. 1 shows ECT sample with following dimensions: L=100mm, B=65mm and h=2.4mm and Lamina properties are present in Table I. Samples were made in five crack length as a_0= 10, 15, 20, 25, 30 mm. An universal testing machine (GOTECH AL-7000L) with 10kN load cell, was used to apply loads in all tests considering displacement controlled. Each test was performed at room temperature, with the crosshead velocity of 0.5mm.min^{-1}. This slow rate allowed crack propagation to be stable and recorded easily.

B. Test Fixture

In the original ECT test fixture (OECT) the specimen was supported at two corners with two support pins, fixed in the other corner by a screw and loaded by a transverse load P at the remaining corner via a fourth pin [2], [7]. In the modified ECT test, employed in this study, the specimens were placed on two support pins positioned at diagonally opposite corners

F. Asgari Mehrabadi is M.Sc. with the University of Tabriz, Faculty of Mechanical Eng., 51666, Tabriz, Iran (e-mail: f.asgari88@ms.tabrizu.ac.ir).
M.R. Khoshravan is Associate Professor with the University of Tabriz, Faculty of Mechanical Engineering, 51666, Tabriz, Iran. (Corresponding author; phone: +98.411.2484; e-mail: rkhosh@tabrizu.ac.ir).

and loaded by two pins located at the two remaining corners attached to load frame. In spite of original ECT test fixture, in modified ECT test, the load is equally distributed to the ECT specimen.

The Load P and crosshead displacement δ are recorded during each test using date acquisition software on a computer connected to the test machine. The test is performed until the propagation of an initial crack. The specimen compliance C is calculated by taking the slope of the load-displacement plot. Load and support pin spans are shown in Fig. 1 with following dimensions: d=80mm and e=35mm.

TABLE I
LAMINA ELASTIC PROPERTIES

	E_x	E_y	E_z	G_{xy}	ν
Woven GFRP	22(GPa)	5(GPa)	19.5(GPa)	4(GPa)	0.3

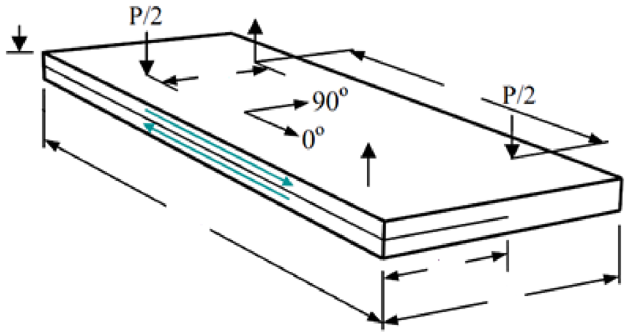

Fig. 1 Schematic diagram of ECT test for mode III delamination

III. Data Reduction

Naturally, data reduction in ECT tests is more complex than in modes I and II fracture tests. The first analysis by Lee [7] applied the mechanics of materials moment-rotation relation to the delaminated and non-delaminated parts of the specimen, and used Classical Lamination Theory (CLT) to derive the torsional stiffness of each part. Compliance and fracture toughness are calculated using the following expressions:

$$C = \frac{\delta}{P} = \frac{e^2 d}{4\{B - (1-2s)a\}(\mu_{xy})_0} \tag{1}$$

$$J_{IIIC} = \frac{P_C{}^2 C(1-2s)}{2eB\{1-(1-2s)(a/B)\}} \tag{2}$$

where, e is moment arm length, d is effective specimen length, B is specimen width, a is initial crack length, P_c is critical load, $(\mu_{xy})_0$ and $(\mu_{xy})_I$ are torsional stiffness terms for the un-cracked laminated and cracked half laminate, $s = (\mu_{xy})_0/(\mu_{xy})_I$.

In this paper, the method is called CC method. Compliance of each specimen is plotted as a function of crack length. Linear regression analysis is performed to determine the constants, A and m.

Compliance and fracture toughness are calculated using the following expressions:

$$\frac{1}{C} = A - m\,a \tag{3}$$

$$J_{IIIC} = \frac{P^2}{2B}\frac{dc}{da} = \frac{mP^2}{2C(A-ma)^2} \tag{4}$$

IV. Finite Element Method

Three dimensional finite element analyses is performed to calculate the compliance, the distribution of mode I, mode II, and mode III energy release rate along the delamination front. Three dimensional finite element models with five different crack lengths are constructed using the ANSYS 12.

Probably the most commonly employed fracture mechanics based approach in predictive failure analysis of composite structures is the virtual crack closure technique (VCCT). The technique and its applications are extensively covered by Krueger [9]. The VCCT methodology, which requires only single FE analysis, is based on the assumption that the energy released when a crack is extended is identical to the energy required to close the crack. Additionally, the single-step method also presumes that a crack extension of Δa does not significantly alter the state of the crack tip. The technique uses nodal forces at the delamination front and the displacements behind the delamination front to determine the strain energy release rate (SERR) components. The energy release rate is calculated using the following expressions:

$$J_{\mathrm{I}} = -\frac{1}{2\Delta A}.Z_{Li}.(w_{L\ell} - w_{L\ell^*}) \tag{5}$$

$$J_{\mathrm{II}} = -\frac{1}{2\Delta A}.X_{Li}.(u_{L\ell} - u_{L\ell^*}) \tag{6}$$

$$J_{\mathrm{III}} = -\frac{1}{2\Delta A}.Y_{Li}.(v_{L\ell} - v_{L\ell^*}) \tag{7}$$

Fig.2 contains an illustration of the delamination front elements typical in the finite element models of the ECT specimens. Where ΔA is the virtually closed area; X_{Li}, Y_{Li} and Z_{Li} are the forces at the crack front in global x, y and z-directions, respectively.

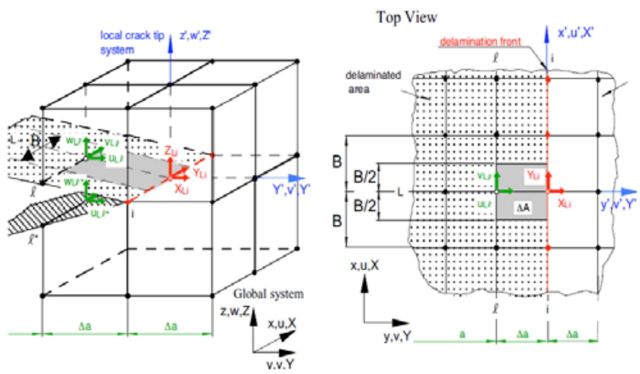

Fig. 2 Delamination front region of finite element models

Corresponding global displacements behind the crack front at the upper sub-laminate are denoted as u_{Li} ,v_{Li} and w_{Li} , whereas displacement at the lower sub laminate are designated as u_{Li*}, v_{Li*} and w_{Li*}. Geometrically nonlinear analysis is performed. The edge crack is modeled by introducing elements with double nodes on the plane of the crack (contact elements). The eight-node solid elements are used and the numbers of elements of the model without contact elements and with contact elements are 15890 and 16920, respectively. Material properties used are shown in Table I. All dimensions and boundary conditions are similar to the real experimental set-up, in order to provide acceptable comparisons (Fig.3).

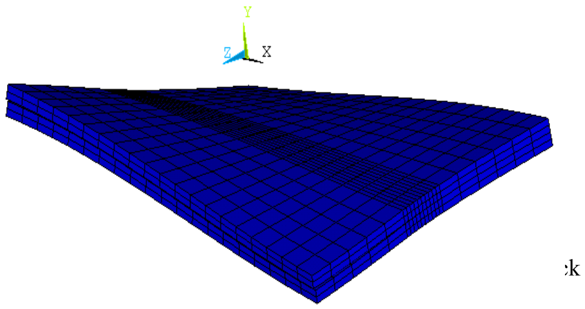

Fig. 3 FE model of an ECT specimen in the deformed configuration

V. Results and Discussion

A. ECT Test

Load-displacement curves are recorded during each test using date acquisition software on a computer connected to the test machine. For mode III loading conditions at least three specimens were tested of each crack length. Load-displacement procedure was performed by a linear response, after which the load-displacement response deviated from linearity. In most cases, the load reached a peak value, followed by a sudden load drop that was assumed to correspond to specimen failure. A load displacement response typical from tests on mode III loading condition is given in Fig. 4. During the tests, stable crack growth was observed at room temperature and there was no stick-slip phenomenon at all tests.

Typically, the fracture test method requires obtaining three critical strain energy release rate values as follows:

(i) J_{IIIC} *(NL)*: the toughness corresponding to load at start of nonlinearity.

(ii) J_{IIC} *(5%/max)*: corresponds to the point where a line 5% offset of the slope intersect the load displacement curve or the maximum load point, whichever occurs first.

(iii) J_{IIIC} *(VIS)*: corresponds to the point where the actual crack initiation is visually observed by the testing personnel.

It should be mentioned that, ECT specimens have a major drawback that because of non-uniform deformed shape geometry, they don't allow visual checking of damage (initiation of crack growth) easily. Therefore, in this study, non-linear (NL) and maximum (5% offset) load points were considered as failure criteria.

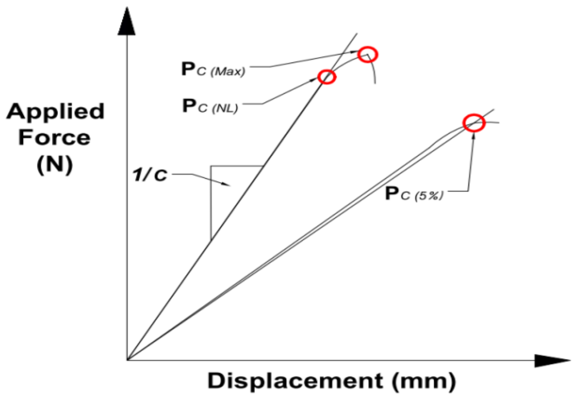

Fig. 4 Typical load-displacement responses from ECT tests

The average values of critical loads were extracted as it is shown in Table II based on non-linear and peak load criteria. As we can found out of Table B, deviation from linearity, P_C (NL), ranged about from 60% to 95% of the maximum loads and the extent of deviation from linearity was found to increase with increasing crack length. Fig. 5 shows compliance results for ECT test obtained by experiment. Linear regression analysis was performed to determine the constants, *A* and *m* of the Eq. (4) for specimen stiffness.

TABLE II
Average Critical Fracture Loads PC (N) for Woven Glass/Epoxy Laminate with Different Crack Length

Critical load (*N*)	Test	Crack length (mm)				
		10	15	20	25	30
	1	1473	1360	1290	1210	790
Max. point	2	1390	1403	1276	1285	1100
	3	1412	1324	1329	1097	805
Average		1424	1362	1298.3	1197	898
	1	1410	1329	1123	855	458
Non-linearity	2	1385	1319	990	923	609
	3	1399.5	1267	1244	765	465
Average		1398.2	1306	1119	847	510.7

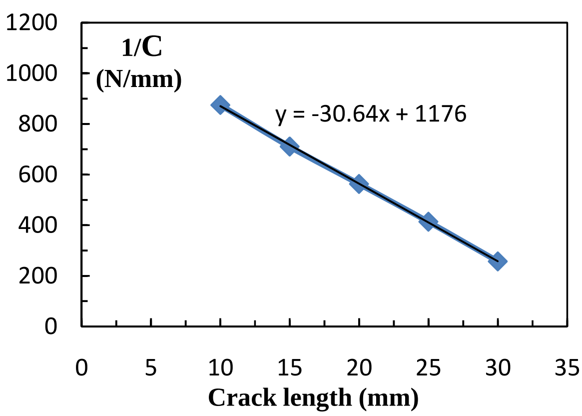

Fig. 5 Specimen stiffness versus crack length

Specimens were then cut along the mid-section and with the help of high resolution digital camera, confirmed delamination and crack growth path, as exemplified in Fig. 6.

Fig. 6 Optical picture of the mid-section of an ECT tested specimen

B. FE Analysis

The effective damage monitoring for this kind of test, depends largely on the accurate prediction or estimation of mechanical behaviors of composite panels. It is difficult to obtain accurate exact solutions for multi-layered panels. Thus, computational approaches like finite element methods play an important role in detecting damage for laminated composites. In this section, the loads corresponding to crack initiation in the ECT specimen were used to calculate the critical strain energy release rates through width of specimen, using nonlinear elastic finite element models. Liao and Sun [8] showed the effect of friction in the ECT test can be ignored, so numerical analyses were done with frictionless contact. In order to definite explanation of initial crack length dependency of J_{IIIc} in the ECT test several aspects intrinsic to the ECT test were analyzed. The first issue examined was the strain energy release rates distribution along the crack front. Fig. 7 presents the distribution of J_{III}, J_{II} and J_{I} normalized by the maximum value of J_{III} for two crack lengths. Almost, in all of crack lengths, the mode I component was verified to be negligible and can be neglect. Also, the mode II component is confined to the limiting region of the pins and it is significantly smaller than the mode III component. An examination of the plots indicates a slight increase of the plateau values with the crack length.

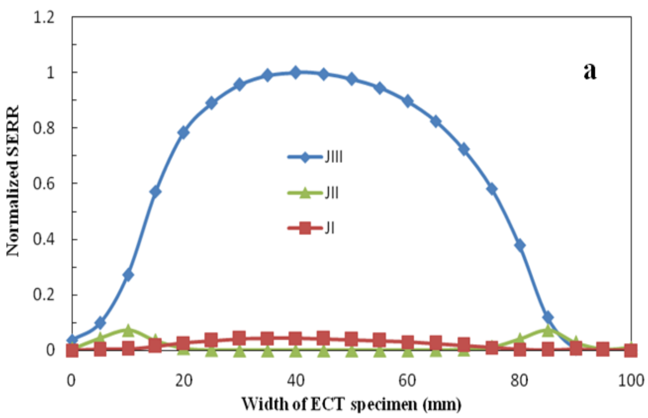

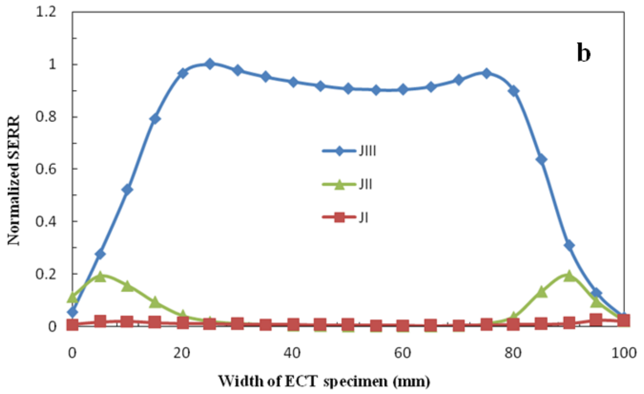

Fig. 7 SERR values obtained by VCCT approach within the different crack lengths through width of ECT specimens. a) 10mm, b) 25mm

VI. CONCLUSION

On the basis of the investigations conducted of mode III delamination behavior of Woven fabric-reinforced glass/epoxy composite laminates at room temperature, using ECT specimens, the following can be concluded:

1- Existing methods for the interpretation of fracture mechanics data, such as the CC and VCCT, proved applicable in the case of ECT test. Their accuracy, however, depends on their ability to accurately describe stiffness degradation during crack propagation.

2- The proposed fixture (modified ECT test) could be very useful for creating of mode III crack growth condition, for any orthotropic or fiber-reinforced material system.

3- It is shown that J_{III} increases with the crack length increase considering two critical points such as $J_{III(NL)}$, $J_{III(Max/5\%)}$ and evaluation of J_{IIIC} by both criteria considered in this study, non-linear point gives conservative and reasonable values than maximum point.

4- By using FEM, it is found that mode III energy release rate is the largest component and that pure mode III is realized within the inner region and Mode II component appears to the neighboring region of the pins.

REFERENCES

[1] Becht G and Gillespie JRJW. Design and analysis of the crack rail shear specimen for mode III interlaminar fracture. *Compos Sci Technol*. 1988; 31: 143–57.

[2] Donaldson SL. Mode III interlaminar fracture characterization of composite materials. *Compos Sci Technol*. 1988; 32: 225–49.

[3] Hwang S-F and Hu C-L. Tearing mode interlaminar fracture toughness of composite materials. *Polym. Compos*. 2001; 22: 57–64.

[4] Sharif F, Kortschot MT, Martin RH. Mode III delamination using a split cantilever beam. In: Martin, R.H. (Ed.), Composite Materials: Fatigue and Fracture. ASTM STP 1230, ASTM, Philadelphia. 1995; 5: 85–99.

[5] Trakas K, Kortschot MT. The relationship between critical strain energy release rate and fracture mode multidirectional carbon fiber/epoxy laminates. In: Armanios, E.A. (Ed.), Composite Materials: Fatigue and Fracture, ASTM STP 1285, ASTM, 1997; 6: 283–304.

[6] Szekrényes A. Improved analysis of the modified split-cantilever beam for mode-III fracture. *Int. J. Mech. Sci*. 2009; 51: 682–93.

[7] Lee SM. An edge crack torsion method for mode III delamination fracture testing. *J Compos Technol Res*. 1993; 15: 193–201.

[8] Liao WC and Sun CT. The determination of mode III fracture toughness in thick composite laminates. *Compos Sci Technol*. 1996; 56: 489–99.

[9] Krueger R. The virtual crack-closure technique: history, approach and applications. ICASE report 2002-10. NASA/CR-2002-211628.